Variable Orbital Coupling in a Two-Dimensional Quantum-Dot Solid Probed on a Local Scale

Peter Liljeroth,[1,*] Karin Overgaag,[1] Ana Urbieta,[2] Bruno Grandidier,[2] Stephen G. Hickey,[3] and Daniël Vanmaekelbergh[1]

[1]*Condensed Matter and Interfaces, Debye Institute, University of Utrecht, PO Box 80000, 3508 TA Utrecht, The Netherlands*

[2]*Département ISEN, IEMN 41 bd Vauban, 59046 Lille Cedex, France*

[3]*Institute of Physical Chemistry, University of Hamburg, Grindelallee 117, D-20146 Hamburg, Germany*

(Received 17 May 2006; published 1 September 2006; corrected 20 October 2006)

The optoelectronic properties of semiconductor quantum-dot (QD) solids depend on the electronic structure of the building blocks and their interactions. Disorder may affect the coupling on a local scale. We have measured the density of states of 2D arrays of PbSe QDs site by site using scanning tunneling spectroscopy. It markedly differs from that of isolated QDs due to electronic coupling in the array. We observe strong local variations in the coupling strength with two prototypical cases: delocalization of the conduction electrons only, and full coupling with both hole and electron delocalization over the QD sites in the array.

DOI: 10.1103/PhysRevLett.97.096803 PACS numbers: 73.22.−f, 73.63.−b, 81.07.−b

Extended systems formed by self-assembly of colloidal semiconductor nanocrystals are often compared to solids built from ordinary atoms [1–6]. Strong confinement of electrons and holes within an isolated nanocrystal host leads to widely spaced, discrete energy levels with atomlike symmetries (*S*, *P*, etc.). Such quantum dots (QDs) can self-assemble to give extended arrays, called nanocrystal superlattices or QD solids [2,7,8], in which the confinement of carriers can be relaxed by quantum mechanical coupling between the QDs [4,9,10]. The optical and electrical properties of these systems are determined by the electronic structure of the nanocrystal building blocks and their mutual interactions; this offers enormous versatility in the design of novel materials with tailored optical, electrical, and magnetic properties. However, unlike ordinary atoms, nanocrystal building blocks suffer from an inherent variation in their size and shape, and are furthermore faceted [2,11]. Unavoidably, there is a loss of translational and orientational order in QD solids [12], which will cause local variations in the electronic coupling. In fact, this is very similar to ordinary glasses where the local structure strongly influences the optical and electrical properties. Macroscopic properties of QD solids, such as electronic conductivity, reflect a system average and overlook microscopic variations [4,5,9,13,14]. Hence, there is a need for measurement of the local electronic structure of the solid on the relevant length scale.

Scanning tunneling microscopy (STM) and spectroscopy (STS) can measure the density of states (DOS) at extremely high spatial resolution and they have been extensively used to measure the electronic structure of single semiconductor QDs and molecules [15–21]. In coupled arrays, only 2D superlattices of Ag nanocrystals have been studied. In that case, the ''atoms'' have a high DOS at the Fermi energy; quantum mechanical coupling is revealed by the disappearance of single-electron charging (Coulomb blockade) [8,22]. In contrast, semiconductor QDs in the strong confinement regime have widely spaced, discrete energy levels; quantum mechanical coupling should markedly affect the DOS. In addition, a reduction in the band gap due to electron and hole delocalization is expected. Superlattices of semiconducting PbSe QDs are good candidates for observing quantum mechanical coupling due to the low effective masses of both the electron and hole [23–25]. This leads to an increased spatial extension of the wave functions of the carriers outside the nanocrystal host, enhancing the electronic coupling between adjacent QDs.

In this Letter, we investigate the local density of states (LDOS) of 2D arrays of semiconductor PbSe QDs by low-temperature STM and STS. The LDOS measured at different sites in the QD lattice is markedly different from that of a single, isolated PbSe QD due to electronic coupling in the array. We report strong microscopic variations in the degree of electronic coupling with two prototypical cases: (i) band-selective coupling, with electron delocalization over neighboring QDs but hole localization, and (ii) full coupling with both electron and hole delocalization and a strongly reduced gap between the highest occupied (HOMO) and lowest unoccupied (LUMO) molecular orbitals.

PbSe QDs capped with oleic acid (molecule length ca. 2 nm) with core diameters of 5.3 nm (±10%) and 7.3 nm (± 5%) were assembled on Au substrates by drop-casting from $CHCl_3$ and vacuum annealed to 120–150 °C in ultrahigh vacuum (UHV) overnight prior to STM experiments [7]. Vacuum annealing leads to interdigitation of the capping molecules as evidenced by the very good stability of the QD arrays under STM imaging and the small interparticle separations [4]. All STM measurements were carried out at 5 K with an UHV STM (Omicron LT-STM). Typical imaging parameters and stabilization settings for spectroscopy were 30 pA/2.5 V and 150 pA/1.2 V, respectively. The spectral features were independent of the set point confirming shell-tunneling conditions [17,26]. The dI/dV spectra were acquired directly with lock-in detection

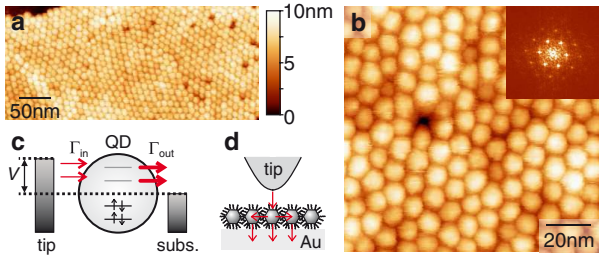

FIG. 1 (color online). (a) Typical large-scale STM topography of 7.3 nm diameter PbSe QDs (array 1). (b) A zoom-in on a domain with quasihexagonal order. Inset: Fourier-transform of the data. (c) Schematic of resonant tunneling spectroscopy in the shell-tunneling regime: the tunneling rate into the QD, Γ_{in}, is much smaller than the tunneling rate out of the QD, Γ_{out}. (d) Relevant tunneling processes in the experiments involving coupled QDs in an array.

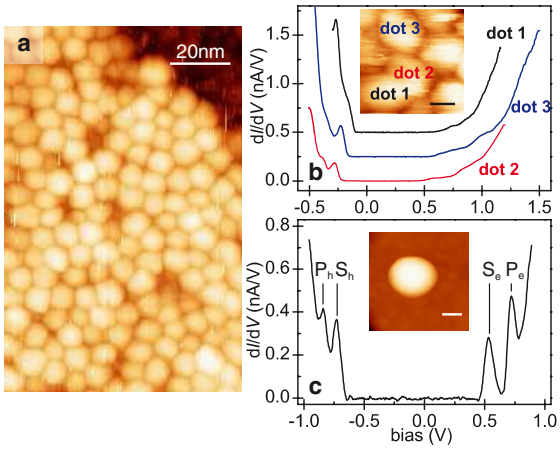

FIG. 2 (color online). Examples of measured dI/dV spectra on neighboring QDs. (a) Large-scale topographic image of 5.3 nm diameter PbSe QDs (array 2). (b) Experimental dI/dV spectra measured on the three neighboring QDs (inset). (c) Spectrum of an isolated PbSe QD (5.3 nm diameter) linked to Au(111) using hexanedithiol. The quantum-confined energy levels corresponding to the tunneling resonances are indicated. Scale bar 5 nm (insets).

(6 mV rms at 1 kHz) and averaged (~100 spectra) to improve signal to noise ratio.

Figure 1(a) shows a topographic image of a 2D array of 7.3 nm PbSe QDs on a Au(111) substrate (array 1). The layer shows local hexagonal packing, but lacks true long-range order due to size and shape dispersion of the nanocrystal building blocks and, probably, also due to orientational disorder of the individual QDs. Figure 1(b) shows a higher magnification image displaying a typical crystalline defect (vacancy) that we often observe in these arrays. The Fourier transform (inset) confirms the presence of quasihexagonal ordering and gives 8.6 nm as the center-to-center spacing corresponding to ~1 nm spacing between the QDs. After topographic imaging, we can select any QD site in the array for tunneling spectroscopy. In shell-tunneling spectroscopy, Fig. 1(c), the tunneling rate into the nanostructure (Γ_{in}) is much smaller than the rate of tunneling out (Γ_{out}) [15,17]. The electrons tunnel through the QD one by one, charging effects are absent, and the measured dI/dV spectrum directly reflects the LDOS at the position of the STM tip. Figure 1(d) shows the relevant tunneling processes in STS on coupled QDs; in order to be able to observe the coupling between the QDs, it has to be larger than the tunneling coupling to the tip or the substrate. In the shell-tunneling regime, Γ_{in} is determined by the set-point current; for typical current values, the resulting coupling energy $h\Gamma_{in}$ is very small, $\sim\mu$eV. The coupling of the QD with the substrate is of the same order of magnitude. Hence, even modest coupling can in principle be observed by STS.

A topographic image of an array of 5.3 nm diameter PbSe QDs is shown in Fig. 2(a) (array 2). The order is less prominent than in Fig. 1, but locally the particles show hexagonal order with an average center-to-center distance of 6.7 nm. The tunneling spectra shown in Fig. 2(b) were measured on three neighboring QDs (inset). The spectra exhibit a zero-conductance gap and resonances resulting from tunneling through valence (negative bias) and conduction levels (positive bias). These spectra can be compared to the spectrum obtained for an isolated PbSe QD depicted in Fig. 2(c) [24]. While the peak at negative bias corresponding to tunneling through the valence S_h level is also observed in the array, the resonances at positive bias on QD sites in the array are significantly broader. This is not due to coupling between the QDs and the gold substrate: an additional self-assembled monolayer (SAM) (hexane- or octanethiol) on Au, to increase the distance between the QDs and the substrate, did not affect the observed broadening in the spectra. These results indicate quantum mechanical coupling between the PbSe QDs in the array. Spectra on neighboring QDs in Fig. 2(b) show very similar features, with only quantitative differences. Such a correlation can be expected if these QDs each form a lattice site in a quantum mechanically coupled island in the array.

We have performed STS on several arrays of PbSe QDs, with diameters of 5.3 nm and 7.3 nm. On each array, we have measured the LDOS on neighboring QD lattice sites, and we have also inspected different regions in each array. In general, we have observed qualitative and quantitative differences in the LDOS with two prototypical cases. Three examples of the more common case measured on three different samples are shown in Fig. 3(a) (three lower spectra). They show peaks at negative bias corresponding to tunneling through the discrete valence levels, while features at positive bias are significantly broadened. The second case, shown in Fig. 3(b), is characterized by steplike features at both positive and negative bias and a significantly reduced width of the zero-conductance gap. Sites in a region with long-range

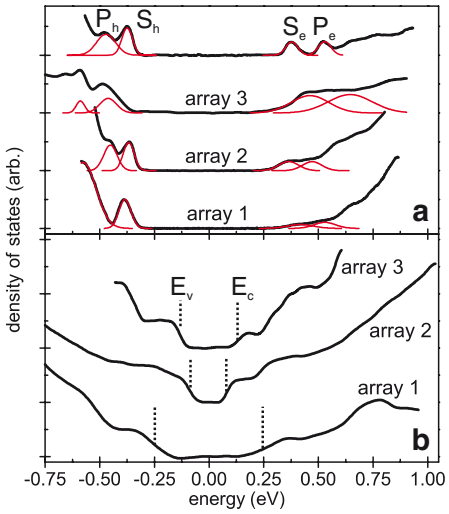

FIG. 3 (color online). Prototypical LDOS measured on PbSe QD sites in an array. (a) Most commonly observed case (three lower spectra). The spectra were measured on three different samples, 7.3 nm diameter QDs (array 1), 5.3 nm QDs (array 2), and 5.3 nm QDs with an additional octanethiol SAM in between the PbSe QDs and the gold substrate (array 3). The top spectrum is that of an isolated 5.3 nm diameter PbSe QD linked to Au(111) using hexanedithiol. The thin lines are Gaussian fits to the first two conduction and valence band features. (b) Examples of spectra in the full coupling regime. Spectra were measured on the same samples as in (a). The conduction and valence band edges are labeled by E_c and E_v, respectively. Bias voltage, V, converted to energy scale using $\eta = (V_{\mathrm{QD}} - V_{\mathrm{tip}})/V = 0.85$ and the DOS taken as the normalized differential conductance $d\ln I/d\ln V$ and normalized with respect to the height of the first valence level (band).

order (array 1) did not show a significantly different spectroscopic response compared to those in regions with only local order (array 2). This indicates that the changes in the density of states are mostly due to coupling between nearest neighbors.

Gaussians have been fitted to the band edge features of the spectra in Fig. 3(a) to get a quantitative measure of the broadening of the DOS. The full width at half maximum (FWHM) for the isolated QD is 65 meV for S_e and 59 meV for S_h. This linewidth is partly due to the lifting of the degeneracy of $S_{e/h}$ states in PbSe QDs [23,24]. The QDs in arrays have similar widths for the first valence level; however, the first conduction resonance has a significantly larger FWHM: 206 (array 3), 106 (array 2), and 138 meV (array 1). We will consider the coupling strength in more detail and compare it with quantum mechanical calculations below. The implication of the spectra shown in Fig. 3(a) is that band-selective coupling between the QDs predominates in the arrays: valence orbitals are not or only weakly coupled while the conduction levels couple with a strength (defined as the extra broadening of the DOS features) of 50–150 meV.

On a considerable minority of lattice sites in the array, the LDOS is qualitatively different, see Fig. 3(b). The tunneling spectra show steps at both positive and negative bias. The steps in the DOS are a signature of a 2D semiconductor indicating strong quantum mechanical coupling of both electron and hole orbitals of adjacent PbSe QDs. Because of the delocalization of the electron and hole wave functions in the plane of the array, the confinement energy is strongly reduced, which is seen as a considerable reduction of the HOMO-LUMO gap with respect to that of a single, isolated PbSe QD. From these spectra reflecting full coupling, on average, a band gap of 300 meV is obtained. The band gap of isolated PbSe QDs is 750 meV [based on STS measurements [24]]. Since the bulk band gap of PbSe at $T = 5$ K is 145 meV, the confinement energy is reduced from 600 meV to ca. 150 meV. We conclude that about $2/3$ of the confinement energy is lost due to delocalization of the electron and hole wave functions. This is consistent with the formation of a 2D electronic system from zero-dimensional building blocks.

The LDOS measured at the QD sites in an array is essentially different from that of isolated PbSe QDs. We offer further support for these findings with quantum me-

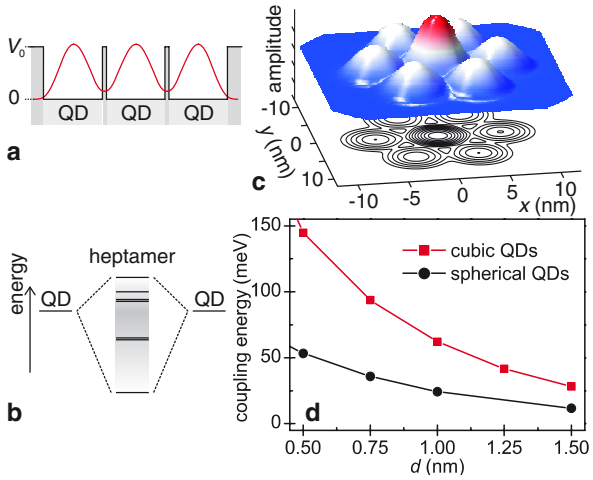

FIG. 4 (color online). Schematic of the level hybridization and results from effective-mass calculations of the ground-state molecular orbital in a QD heptamer. (a) A cross section of the potential energy landscape used in the model along the center of the QD heptamer. (b) Splitting of the QD levels due to quantum mechanical coupling between the QDs: lines indicate the energy level positions in a QD heptamer. In the limit of a large number of coupled QDs, a miniband would be formed. (c) The amplitude of the ground-state wave function in a QD heptamer showing delocalization and formation of a molecular orbital. (d) Calculated coupling energy (defined as the splitting between the most bonding and antibonding orbital) as a function of the nanocrystal edge-to-edge separation for both spherical (black spheres) and cubic QDs (red boxes). The effective mass was 0.05, the barrier height between the QDs 2 eV and the diameter of the spherical QDs was 6 nm; the size of cubic QDs (5 nm) was adjusted to give similar confinement energy.

chanical calculations on PbSe QDs placed in an array. In Fig. 4, we consider a QD heptamer, with seven spherical (or cubic) QDs separated by an energy barrier [Fig. 4(a)]. We solve the Schrödinger equation in the effective-mass approximation and concentrate on the seven lowest energy eigenstates, which arise from the quantum-confined energy levels with *S*-type envelope symmetry. The individual QD wave functions overlap and this results in the formation of molecular orbitals [27,28]. Figure 4(b) shows the resulting energy level structure where the original eigenstates are split due to coupling. Bonding and antibonding molecular (superlattice) orbitals are formed; the ground-state wave function is shown in Fig. 4(c). The orbital is delocalized over all the QDs in the heptamer. Figure 4(d) shows the calculated coupling energies (defined as the splitting between the most bonding and antibonding orbitals) which are of the order of 50 meV for realistic nanocrystal separations. The nanocrystal symmetry is important: the calculated coupling energy is a factor of 3 higher for cubic nanocrystals. This is due to the enhanced wave-function overlap between the neighboring QDs due to the nanocrystal facets. Our experiments were performed with faceted nanocrystals with an overall spherical shape; the coupling strength is likely to be intermediate between the values calculated for the spherical and cubic nanocrystals. In addition, we have found that rotation of the central nanocrystal in the heptamer of cubic QDs (while keeping the nanocrystal edge-to-edge separation constant) can lead to a reduction of the coupling energy of up to 75%. Finally, calculations on larger assemblies (up to 7×7 dots, fixed edge-to-edge separation of 1 nm) allow extrapolation of coupling energies to infinite systems: this gives for hexagonal arrays of spherical and cubic QDs 38 meV and 99 meV, respectively, and 132 meV for square arrays of cubic QDs.

As the effective masses of the electrons and holes are very similar in PbSe, the observed band-selective orbital coupling is surprising. The most plausible explanation for the band-selective coupling is a variation in the potential landscape experienced by electrons and holes. It has been observed that the nonresonant LUMO (HOMO) orbitals of the barrier material can have a strong influence on the effective barrier height for electron (hole) tunneling [29]. It is possible that the oleic acid LUMO orbitals enhance electron tunneling between adjacent QDs more than the HOMO orbitals do for holes. We remark that Talapin and Murray performed long-range transport measurements on PbSe QD solids and report a sixfold higher mobility for electrons than for holes, in qualitative agreement with our results [14]. According to the calculations, a difference of 1–2 eV in the effective barrier height is sufficient to explain the observed difference in the coupling strength. The simple model used here can explain the coupling strength that is measured in most regions in the arrays. However, more realistic methods, such as tight-binding or pseudopotential calculations will be required for a full understanding of our experiments.

In summary, we have shown that measurements on a local scale are vital in providing detailed knowledge on the strength and nature of quantum mechanical coupling in inherently disordered arrays of colloidal QDs. STS measurements on 2D arrays of PbSe QDs show that the individual QDs are predominantly coupled in a band-selective fashion with a coupling strength of 50–150 meV between the conduction levels. In addition, some regions of the array display strong coupling of both the conduction and valence levels. Local variations in the electronic structure should not be overlooked in the design of QD materials with tailored properties.

The authors thank A. Houtepen, R. Koole, J. Kelly, and P. Zeijlmans van Emmichoven for discussions. Financial support from the EU (RTN "NANOSPECTRA", HPRH-CT-2001-00320) is acknowledged.

*Electronic address: P.Liljeroth@phys.uu.nl

[1] M. A. Kastner, Phys. Today **46**, No. 1, 24 (1993).
[2] C. B. Murray, C. R. Kagan, and M. G. Bawendi, Annu. Rev. Mater. Sci. **30**, 545 (2000).
[3] F. X. Redl *et al.*, Nature (London) **423**, 968 (2003).
[4] H. E. Romero and M. Drndic, Phys. Rev. Lett. **95**, 156801 (2005).
[5] D. Yu, C. Wang, and P. Guyot-Sionnest, Science **300**, 1277 (2003).
[6] E. V. Shevchenko *et al.*, Nature (London) **439**, 55 (2006).
[7] C. B. Murray *et al.*, IBM J. Res. Dev. **45**, 47 (2001).
[8] G. Markovich *et al.*, Acc. Chem. Res. **32**, 415 (1999).
[9] D. Yu *et al.*, Phys. Rev. Lett. **92**, 216802 (2004).
[10] M. V. Artemyev *et al.*, Phys. Rev. B **60**, 1504 (1999).
[11] A. P. Alivisatos, J. Phys. Chem. **100**, 13 226 (1996).
[12] R. P. A. Dullens *et al.*, Phys. Rev. Lett. **96**, 028304 (2006).
[13] A. L. Roest *et al.*, Phys. Rev. Lett. **89**, 036801 (2002).
[14] D. V. Talapin and C. B. Murray, Science **310**, 86 (2005).
[15] U. Banin and O. Millo, Annu. Rev. Phys. Chem. **54**, 465 (2003).
[16] U. Banin *et al.*, Nature (London) **400**, 542 (1999).
[17] E. P. A. M. Bakkers *et al.*, Nano Lett. **1**, 551 (2001).
[18] T. Maltezopoulos *et al.*, Phys. Rev. Lett. **91**, 196804 (2003).
[19] G. V. Nazin, X. H. Qiu, and W. Ho, Phys. Rev. Lett. **95**, 166103 (2005).
[20] A. Wachowiak *et al.*, Science **310**, 468 (2005).
[21] D. Steiner *et al.*, Phys. Rev. Lett. **95**, 056805 (2005).
[22] S. H. Kim *et al.*, J. Phys. Chem. B **103**, 10 341 (1999).
[23] G. Allan and C. Delerue, Phys. Rev. B **70**, 245321 (2004).
[24] P. Liljeroth *et al.*, Phys. Rev. Lett. **95**, 086801 (2005).
[25] F. Wise, Acc. Chem. Res. **33**, 773 (2000).
[26] L. Jdira *et al.*, Phys. Rev. B **73**, 115305 (2006).
[27] M. Bayer *et al.*, Science **291**, 451 (2001).
[28] G. Bester, J. Shumway, and A. Zunger, Phys. Rev. Lett. **93**, 047401 (2004).
[29] W. Wang, T. Lee, and M. A. Reed, Rep. Prog. Phys. **68**, 523 (2005).